ASCE

Sign Constrained Bayesian Inference for Nonstationary Models of Extreme Events

Abhinav Prakash[1]; Vijay Panchang, Ph.D., F.ASCE[2]; Yu Ding, Ph.D.[3]; and Lewis Ntaimo, Ph.D.[4]

Abstract: Recent studies show that many of the extreme events in hydrology can be modeled more realistically by means of a nonstationary generalized extreme value (GEV) distribution. However, existing approaches for estimating the parameters can mistake a positive trend in the data to be negative. This can lead to underdesigning in engineering projects. To address this issue, this work devises a sign constrained Bayesian inference method for nonstationary GEV distributions. This new approach ensures that the final GEV model embodies a trend consistent with the physical understanding of the underlying phenomenon and design requirements. The advantage of using the sign constrained Bayesian approach is twofold: first, it produces a probability distribution instead of a point estimate of the model parameters; and second, it affords a natural method of uncertainty quantification, thus giving greater confidence to engineers in selecting design parameter values for civil and mechanical structures to withstand extreme events. The merit of the proposed Bayesian approach is illustrated using two water level datasets pertaining to tidal rivers in New Jersey. The results show that the new method is capable of appropriately handling datasets for which traditional methods return a positive or negative slope in the location parameters, and produces the posterior distribution of the parameters based on the observed data and not point estimates. Further, the availability of a probability distribution for the return event gives engineering designers and planners additional information and perspective on the risks involved. **DOI: 10.1061/(ASCE)WW.1943-5460.0000589**. *© 2020 American Society of Civil Engineers.*

Introduction

Probabilistic modeling of extreme events is often performed using the generalized extreme value (GEV) distribution or other distributions. such as the Gumbel distribution, the Weibull distribution, etc. Engineers are often interested in understanding the behavior of extreme events to develop a basis for designing civil engineering structures such as floodwalls and bridges. The reliability of these structures is paramount to public safety. For instance, about 40% of the land area in the Netherlands is below sea level (Haan and Ferreira 2006). This portion of land is protected against flooding by construction of storm-surge barriers, which should withstand extreme water levels. These barriers are undergoing renovations, which should be able to withstand oceanic conditions corresponding to a probability of occurrence of 10^{-4} in a given year. Then the question that becomes relevant is the following: How should this probability be translated into a design quantile for the height of the dyke? In statistics, extreme value theory provides techniques for answering this type of question.

The standard form of the GEV distribution is a stationary model, which means that the parameters of the distribution (i.e., the location, scale, and shape parameters) are time invariant. However, hydrological maxima often show time-dependent trends (Potter 1991; Olsen et al. 1999; Lins and Slack 1999; Douglas et al. 2000; Strupczewski et al. 2001b), thus creating a need for probabilistic modeling to incorporate the trends observed in the data. This can be handled by using a nonstationary GEV distribution whose parameters are a function of time (Coles 2001), so that the probability distribution changes over the time. A nonstationary GEV distribution is generally based on prespecified trends in the parameters, enabling one to capture the change in the probability of occurrence of the underlying events over time.

The commonly used technique to estimate the parameters for a nonstationary GEV distribution is the maximum likelihood estimation (MLE) method. Examples include the work of Caires et al. (2006) in the context of significant wave heights; of the studies of Salas and Obeysekera (2014) of peak discharges in the Aberjona River and Sugar Creek Basin; and of the work of Masina and Lamberti (2013) in the context of extreme sea levels in the northern Adriatic (see also Strupczewski et al. 2001a). Conversely, Mudersbach and Jensen (2010) have used the *L*-moments method (Gado and Nguyen 2016) to estimate the 100 year extreme water levels for the North Sea coast. Although the *L*-moments method is valid for stationary distribution, it can be applied to a nonstationary distribution by first detrending the time-series data and then applying the method. The results of Gado and Nguyen (2016) based on simulated datasets suggest that this method can perform as well as or better than the MLE method in most cases. In another related work, the moments method is used to estimate intensity–duration–frequency (IDF) rainfall curves in some African cities (De Paola et al. 2014).

An alternative to the MLE and *L*-moments approaches is the Bayesian inference approach. The Bayesian approach considers the parameters of the GEV distribution as random variables. Therefore, it employs the concept of priors, which reflects the prior belief for any parameter before observing the data and computes a posterior distribution of the parameters based on the given data. The priors can act as a layer of information if some properties of the

[1]Ph.D. Student, Dept. of Industrial and Systems Engineering, Texas A&M Univ., 3131 TAMU, College Station, TX 77843. ORCID: https://orcid.org/0000-0002-1792-8011. Email: abhinavp@tamu.edu

[2]Professor and Program Chair, Dept. of Mechanical Engineering, Texas A&M Univ. at Qatar, Education City, Doha, Qatar. Email: vijay.panchang@qatar.tamu.edu

[3]Professor, Dept. of Industrial and Systems Engineering, Texas A&M Univ., 3131 TAMU, College Station, TX 77843 (corresponding author). Email: yuding@tamu.edu

[4]Professor, Dept. of Industrial and Systems Engineering, Texas A&M Univ., 3131 TAMU, College Station, TX 77843. ORCID: https://orcid.org/0000-0002-9114-5170. Email: ntaimo@tamu.edu

parameters are known, while having a posterior distribution of the parameters offers the benefit of uncertainty quantification. This approach has been taken, for example, to analyze trend-related peak flow attributes of the Wainganga river basin in India (Das and Umamahesh 2017). The work by De Paola et al. (2018) compares the Bayesian method and the MLE method for parameter estimation using both stationary and nonstationary models for extreme rainfall in some African cities.

In spite of the widespread use of these methods, a potential problem appears to have gone unnoticed. Certain datasets of extreme events often exhibit an increasing trend; but, while applying a nonstationary model, these methods produce a negative slope for the location parameter. The problem with this phenomenon is that a negative slope for the location parameter could lead to the underdesign of a structure (since the data points themselves possess an increasing trend). This is illustrated by means of an analysis of data for the Hackensack River in New Jersey. The purpose of this work is to alert the practitioner to this problem and to suggest a remedy. The problem may be solved by using a constrained optimization of the likelihood function but the solution for this optimization problem invariably yields a zero slope for the location parameter, thus rendering the process stationary.

The contribution of this work to nonstationary GEV modeling applications is the development of a sign constrained Bayesian method for parameter estimation problems involving nonstationary phenomenon. The motivation for this work stems from the need to incorporate a physical understanding of the phenomenon in the GEV model to improve estimation. The use of appropriate priors in a Bayesian framework allows such understanding to be added to the model in a natural manner. A further benefit of this Bayesian work is its ability to inherently account for the uncertainty in the model, something that is pressingly needed in extreme value analysis but often remains ignored in the research (Coles 2001).

To demonstrate the problem and the solution, we include two case studies involving hydrological data for extreme flows in two tidal rivers. These data have different structures, as explained in the subsequent sections. The two case studies provide an illustration of how to apply the proposed Bayesian method with practitioners in mind, and demonstrate that this unified framework can handle problems with different data structures. The rest of the paper is organized as follows. The next section describes the fundamentals of nonstationary modeling in relation to the GEV distribution. After this, the details of the proposed Bayesian method for parameter estimation are provided and results are reported of the traditional MLE, the constrained MLE, the traditional Bayesian, and the proposed sign constrained Bayesian methods applied to two hydrological datasets. The discourse ends with a summary and concluding remarks.

GEV Distribution for Nonstationary Models

The stationary GEV distribution uses three parameters, namely, the *location* parameter μ, the *scale* parameter σ, and the *shape* parameter ξ. The cumulative distribution function (CDF) for a GEV distribution can be expressed as

$$F(z) = \exp\left(-\left\{1 + \xi\left[\frac{z-\mu}{\sigma}\right]\right\}^{1/\xi}\right) \quad (1)$$

where z = variable associated with the underlying random process, say the value of the water level. The GEV distribution can be modified to incorporate the nonstationarity present in the data by expressing the parameters as functions of time (Coles 2001). The structure of the time dependence can be assumed based on the

pattern of the trends in the data. If, for example, it is assumed that the parameters vary linearly with time, we can write each parameter as a linear function of time t in the following manner:

$$\mu(t) = \mu_0 + \mu_1 t, \qquad \sigma(t) = \sigma_0 + \sigma_1 t, \qquad \xi(t) = \xi_0 + \xi_1 t \quad (2)$$

where $\mu(t)$ = linear function for the location parameter, with intercept μ_0 and slope μ_1; $\sigma(t)$ = function for the scale parameter, with intercept σ_0 and slope σ_1; and $\xi(t)$ = function for the shape parameter, with ξ_0 and ξ_1 as intercept and slope, respectively. It is evident that the number of parameters for a nonstationary model has doubled to six. This makes the resulting model more complicated, and sometimes unnecessarily flexible, creating identifiability issues in parameter estimates. Intuitively, these issues arise when there is an excessive number of parameters in a model and various combinations of the parameters may have the same effect, making it difficult to estimate the parameters uniquely. For this reason, often only the location parameter is regarded as a function of time, while keeping the scale and shape parameters as time-independent constants (e.g., Obeysekera et al. 2013). Such a model, with a linear trend in the location parameter, means that the distribution is shifting linearly with time without changing the overall structure of the distribution, as illustrated in Fig. 1.

Considering the location parameter as a linear function of time, the CDF can be written as

$$F(z,t) = \exp\left(-\left\{1 + \xi\left[\frac{z-(\mu_0+\mu_1 t)}{\sigma}\right]\right\}^{1/\xi}\right) \quad (3)$$

Hence, four parameters $\{\mu_0, \mu_1, \sigma, \xi\}$ are to be estimated, where μ_0 = intercept of the location parameter; and μ_1 = slope of the location parameter. To estimate these parameters using the method of maximum likelihood, let the likelihood function be written as

$$L(\theta) = \prod_{i=1}^{n} f(z_i : \mu(t), \sigma, \xi) \quad (4)$$

where f = the probability density function (PDF) of the distribution; θ = the parameter set $\{\mu_0, \mu_1, \sigma, \xi\}$; z_i = the ith data point; and n = the total number of data points. Then the parameters $\{\mu_0, \mu_1, \sigma, \xi\}$ can be estimated by maximizing the logarithm of the likelihood function.
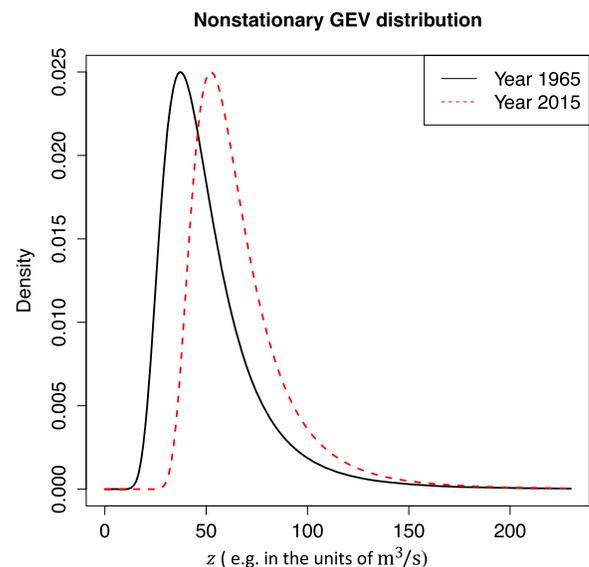
Fig. 1. Example of linear shift in the GEV distribution over time.

For a nonstationary GEV distribution, the time t in the likelihood function is a *variable* and its value depends on the "reference" year selected. If the first data point is considered the reference for constructing the time index, $t = 0, 1, 2, \ldots, n$. Choosing the first available data point as the reference ($t = 0$), however, is just one way to construct the time index (Coles 2001). Any year can, in fact, be taken as the *reference*. The data points preceding the reference would then be modeled as $t = -1, -2, -3\ldots$, while the years succeeding the *reference* year would be modeled as $t = 1, 2, 3\ldots$ For example, Obeysekera and Salas (2016) advocated centering the time variable around the mean of the extreme values and using the mean year as the reference year. The impact of a different reference is that the estimate of the intercept, μ_0, will be affected, but the other parameters will not.

To ensure that the final model is independent of the choice of the reference year, the location intercept must be shifted to reflect the first year of the design life of a structure. Let us call the first year of the design life of a structure the "design" year, y_d. We denote by y_r the *reference* year for constructing the time index. If the location parameter is defined as a linear function of time, as in Eq. (2), the value of the location intercept for the design year can be recalculated as

$$\mu_{0d} = \mu_0 + \mu_1(y_d - y_r) \tag{5}$$

where μ_0 is the location intercept corresponding to the reference year and μ_{0d} is the location intercept corresponding to the design year. For extrapolation into the future, the number of years is counted from the design year and, as such, μ_{0d} should accordingly be used in the nonstationary GEV model, as expressed in Eq. (3).

Let us suppose that the parameter values have been estimated. The next step is to calculate a design quantile. In the example noted earlier, the Dutch government has stipulated that the height of the dykes should be sufficient to withstand water levels with a probability of occurrence of as low as 10^{-4} (exceedance probability) in any given year. If we use a nonstationary model, this exceedance probability is a function of time. Let the exceedance probability for an event z at time t be denoted by $p_t(z)$. Then it can be calculated using the CDF of the GEV distribution, as

$$p_t(z) = 1 - F(z; t)$$
$$= 1 - \exp\left(-\left\{1 + \xi\left[\frac{z - (\mu_0 + \mu_1 t)}{\sigma}\right]\right\}^{1/\xi}\right) \tag{6}$$

Alternatively, the return period, defined as the expected waiting time for an event z, is used in the design. We denote the waiting time for an event z by a random variable X. If the realization of this random variable is $X = x$, i.e., the event z occurs at time x, the PDF of this random variable can be expressed as

$$f(x; z) = \left(\prod_{i=1}^{x-1}(1 - p_i(z))\right)p_x(z) \tag{7}$$

where $p_i(z)$ = the time-varying exceedance probability of event z until time $x - 1$; and $p_x(z)$ = the exceedance probability at time x. Specifically, the waiting time follows a geometric distribution. If the GEV distribution is stationary, i.e., the exceedance probability for any event does not change with time, the expected value of the waiting time becomes (Mood et al. 1974)

$$E(X) = T_{\text{stat}} = \frac{1}{p} \tag{8}$$
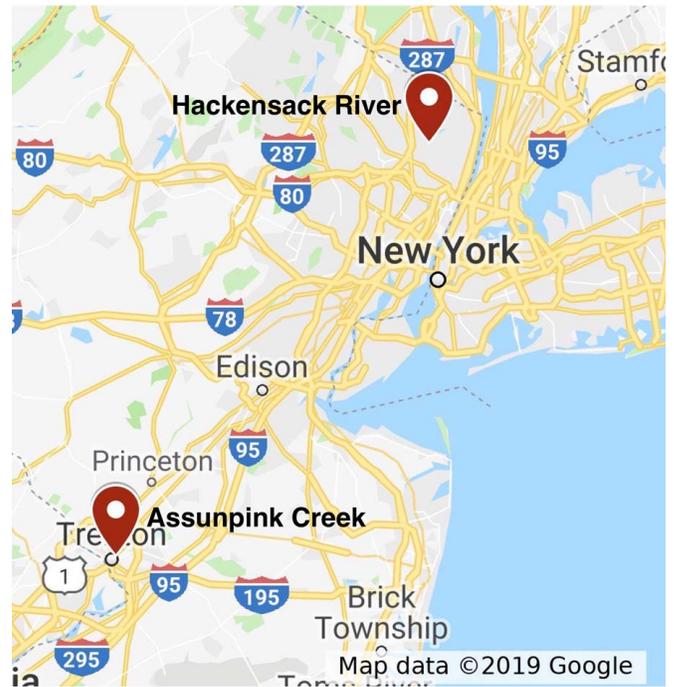
Fig. 2. Location map of the sites used for the case studies. (Map data ©2019 Google.)

where p is the constant exceedance probability for any event z and T_{stat} is the return period for a stationary model.

The formulation for the return period for a nonstationary model is different from that for the stationary one because the exceedance probability is no longer a constant. The concept of return period has been extended by Salas and Obeysekera (2014) for nonstationary hydrologic extreme events. If $p_t(z)$ is the time-varying exceedance probability of event z for time $t = 1, 2, 3\ldots$, the *return period* for event z can be given as

$$T_{\text{nstat}} = 1 + \sum_{x=1}^{x_{\max}}\prod_{t=1}^{x}(1 - p_t(z)) \tag{9}$$

where T_{nstat} = the return period for the nonstationary model; and $x_{\max}$ = a time point such that $p_{x_{\max}}(z) = 1$.

From Eq. (6), it can be seen that the exceedance probability $p_t(z)$ is a function of time and keeps on increasing for a given value of event z if there is a positive trend in the location parameter. Hence, $x_{\max}$ is the time when the exceedance probability of a given event, $p_{x_{\max}}(z)$, reaches one. However, if the location parameter has a negative trend, $p_t(z)$ will keep on decreasing, $p_{x_{\max}}(z)$ will never reach one, and $x_{\max}$ can be considered as ∞ (Salas and Obeysekera 2014). Numerical calculations using $x_{\max}$ as ∞ would give $T_{\text{nstat}} = \infty$, which means that, in practice, if the location parameter has a negative trend, the nonstationary return period calculation becomes meaningless.

One way to approach this problem could be to resort a stationary model whenever the parameter estimate returns a negative slope. The implication is that the structures are designed at least for the current level of extremes. Apparently, this approach leads to an underestimate of the design quantile if there is indeed a positive trend in the occurrence probability of the underlying events. Since this approach does not produce satisfactory outcomes, we propose a "sign constrained" Bayesian approach for parameter estimation, which we describe next.

© ASCE

04020029-3

J. Waterway, Port, Coastal, Ocean Eng.
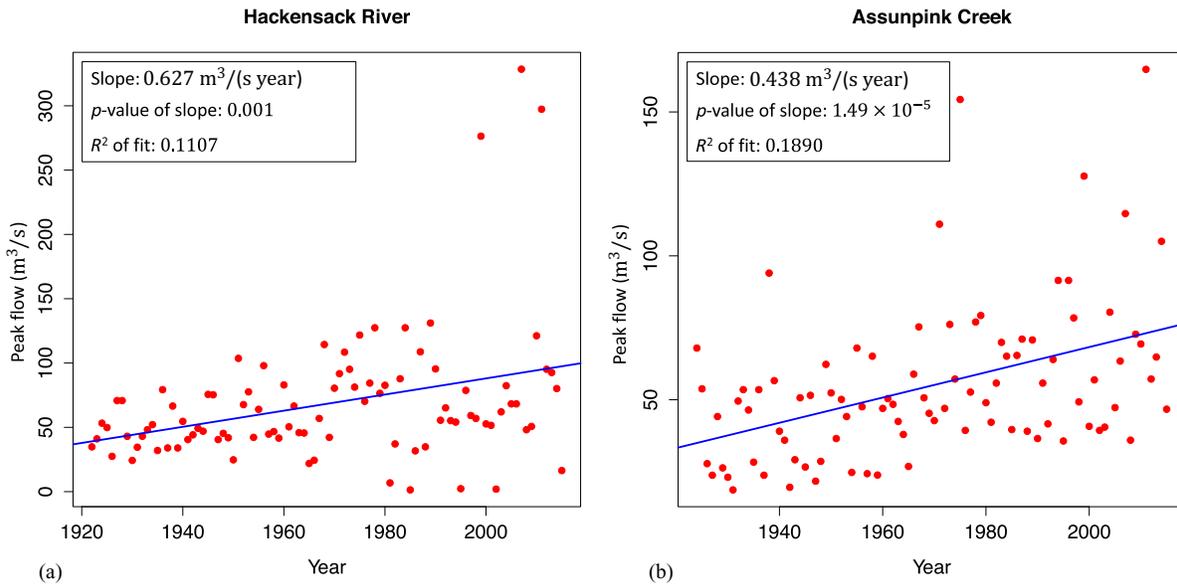
Fig. 3. Annual peak flow data with best linear fit for (a) Hackensack River; and (b) Assunpink Creek.

Sign Constrained Bayesian Method

Let θ be a vector of the parameters of any distribution such that $\theta \in \Theta$, where Θ is the set of all the possible values of the parameters. Let $p(\theta)$ be the *prior* and $p(\theta \mid z)$ be the *posterior* distribution of the parameter θ after observing the data z. *Bayesian inference* allows for learning the posterior from the prior via Bayes' rule (Cox 1946, 1961; Savage 1972):

$$p(\theta \mid z) = \frac{p(z|\theta)p(\theta)}{\int_\Theta p(z|\theta)p(\theta)\, d\theta} \qquad (10)$$

where $p(z|\theta)$ is the likelihood that the data comes from a distribution with given parameter θ. Eq. (10) does not state what a *rational* person's belief should be; it only states how the belief should change in light of the observed data. Hence, the posterior distribution would depend on the prior belief and different priors could result in different posteriors, thus making the analysis dependent on the personal choice of priors. Nevertheless, using priors offers an opportunity to steer the parameter estimation process to be in line with the underlying physical trend.

In Eq. (10), the denominator involves an integration over the parameter space and can become very difficult (or sometimes impossible) to compute as the number of parameters in the model increases. Therefore, approximation schemes for computing the posterior distribution are often availed of; here we resort to the commonly used Markov chain Monte Carlo (MCMC) method. The idea behind the MCMC method is to simulate the posterior distribution by taking a large number of samples from the posterior distribution. We use the Metropolis-Hastings algorithm (Metropolis et al. 1953; Hastings 1970; Hoff 2009) to sample from the posterior distribution. This sampling algorithm constructs a sequence $\{\theta^{(1)}, \theta^{(2)}, \ldots, \theta^{(s)}\}$ such that $\theta \sim p(\theta \mid z)$.

Suppose that a working sequence $\{\theta^{(1)}, \theta^{(2)}, \ldots, \theta^{(s)}\}$ has been constructed and the next value $\theta^{(s+1)}$ must be added. The Metropolis-Hastings algorithm proceeds by sampling a proposed value θ^* close to the current value $\theta^{(s)}$. A *proposal distribution* $J(\theta^* \mid \theta^{(s)})$ is used to obtain θ^*. Generally, a symmetric proposal distribution is used. Common examples include uniform$(\theta^{(s)} - \delta, \theta^{(s)} + \delta)$ and normal$(\theta^{(s)}, \delta^2)$, where δ is known as the *proposal width*.

Table 1. Specifications for the MCMC algorithm

Specification	Assunpink Creek	Hackensack River
Location intercept μ_0 prior	Uniform (0, 200)	Uniform (0, 200)
Location slope μ_1 prior		
SC-BM	Uniform (0, 5)	Uniform (0, 5)
UC-BM	Uniform (−5, 5)	Uniform (−5, 5)
Scale σ prior	Uniform (0, 50)	Uniform (0, 50)
Shape ξ prior	Uniform (−1, 1)	Uniform (−1, 1)
Initial values $\{\mu_0, \mu_1, \sigma, \xi\}$	$\{50, 1, 20, 0.8\}$	$\{50, 1, 20, 0.8\}$
Proposal distributions		
μ_0	Normal (., 1)	Normal (., 2)
μ_1	Normal (., 0.1)	Normal (., 0.15)
σ	Normal (., 1)	Normal (., 1)
ξ	Normal (., 0.05)	Normal (., 0.05)

Table 2. Results for Hackensack River

Method	μ_0	μ_1	σ	ξ	100 year flow (m³/s)	NLLH
SC-BM (MAP)	51.66	0.000	30.72	0.0870	235.7	471.83
SC-BM (expected)	53.11	0.093	31.44	0.0977	246.2	471.72
UC-BM (MAP)	45.54	−0.042	29.76	0.1189	—	471.05
UC-BM (expected)	44.71	−0.048	30.66	0.1385	—	471.28
MLE	45.59	−0.034	29.19	0.1184	—	471.02
C-MLE	47.51	0.000	29.39	0.1093	223.2	471.06

Note: No 100-year return event estimate when slope parameter μ_1 is negative.

Table 3. Results for Assunpink Creek

Method	μ_0	μ_1	σ	ξ	100 year flow (m³/s)	NLLH
SC-BM (MAP)	56.20	0.281	15.33	0.2115	195.2	404.36
SC-BM (expected)	56.55	0.282	15.62	0.2244	214.3	404.32
UC-BM (MAP)	55.53	0.277	14.99	0.1873	194.9	404.40
UC-BM (expected)	56.95	0.286	15.58	0.2047	205.6	404.23
MLE	56.96	0.289	14.86	0.2027	195.1	404.07
C-MLE	56.96	0.289	14.86	0.2027	195.1	404.07

Once the value of θ^* is obtained, the acceptance ratio r is calculated as

$$r = \frac{p(z|\theta^*)p(\theta^*)J(\theta^{(s)}|\theta^*)}{p(z|\theta^{(s)})p(\theta^{(s)})J(\theta^*|\theta^{(s)})} \quad (11)$$

For a symmetric proposal distribution, $J(\theta^{(s)}|\theta^*) = J(\theta^*|\theta^{(s)})$, which simplifies Eq. (11). The intuition behind computing the acceptance ratio is that if the ratio is greater than one, it is more likely that the given data came from a sampling distribution whose parameter is θ^*. Thus, θ^* should be included in the set of samples, $\theta^{(s+1)} = \theta^*$. If the ratio is less than one, the parameter value θ^* should only be included in the set of samples with probability r. If the proposed sample θ^* is rejected, $\theta^{(s+1)} = \theta^{(s)}$.

The algorithm can be summarized as follows.
1. Choose the prior distribution for the parameter and select the initial value of the parameter.
2. Choose the proposal distribution for the parameter.
3. Sample the next value of parameter θ^* based on the current value $\theta^{(s)}$ of the parameter and proposal distribution.
4. Compute the acceptance ratio (r).
5. Accept the proposed sample with probability min (r, 1) and update $\theta^{(s+1)} = \theta^*$; otherwise reject the proposed sample and update $\theta^{(s+1)} = \theta^{(s)}$.

The algorithm converges to the target posterior distribution after the Markov chain or the sequence $\{\theta^{(1)}, \theta^{(2)}, \ldots, \theta^{(s)}\}$ reaches a steady state. Hence, the samples collected before reaching the steady state or during the transient state of the Markov chain (*burn-in samples*) are discarded as they do not represent the target posterior distribution. The number of burn-in samples would vary based on the convergence rate of the algorithm. The convergence rate depends on the nature of the dataset, the initial values of the parameters, the proposal distribution, and the selection of priors. The algorithm can be stopped after a sufficient number of samples from the distribution $p(\theta \mid z)$ has been collected.

The use of informative priors to compute the posterior enables us to constrain some parameters as needed. In this work, if we know that some of the parameters should not take negative values, we impose a nonnegativity constraint when accepting samples using an appropriate prior. We impose a uniform prior with a nonnegative support on the location parameter and the scale parameter (because it is the variance). We refer to the resulting Bayesian method as a *sign-constrained Bayesian method* (SC-BM). We applied the SC-BM to two case studies involving the return level for peak flow of water streams and report the findings in the next section.

Case Studies

We consider two case studies involving data for annual peak flow in rivers and perform a comparative computational study of the proposed Bayesian method and the standard frequentist methods.
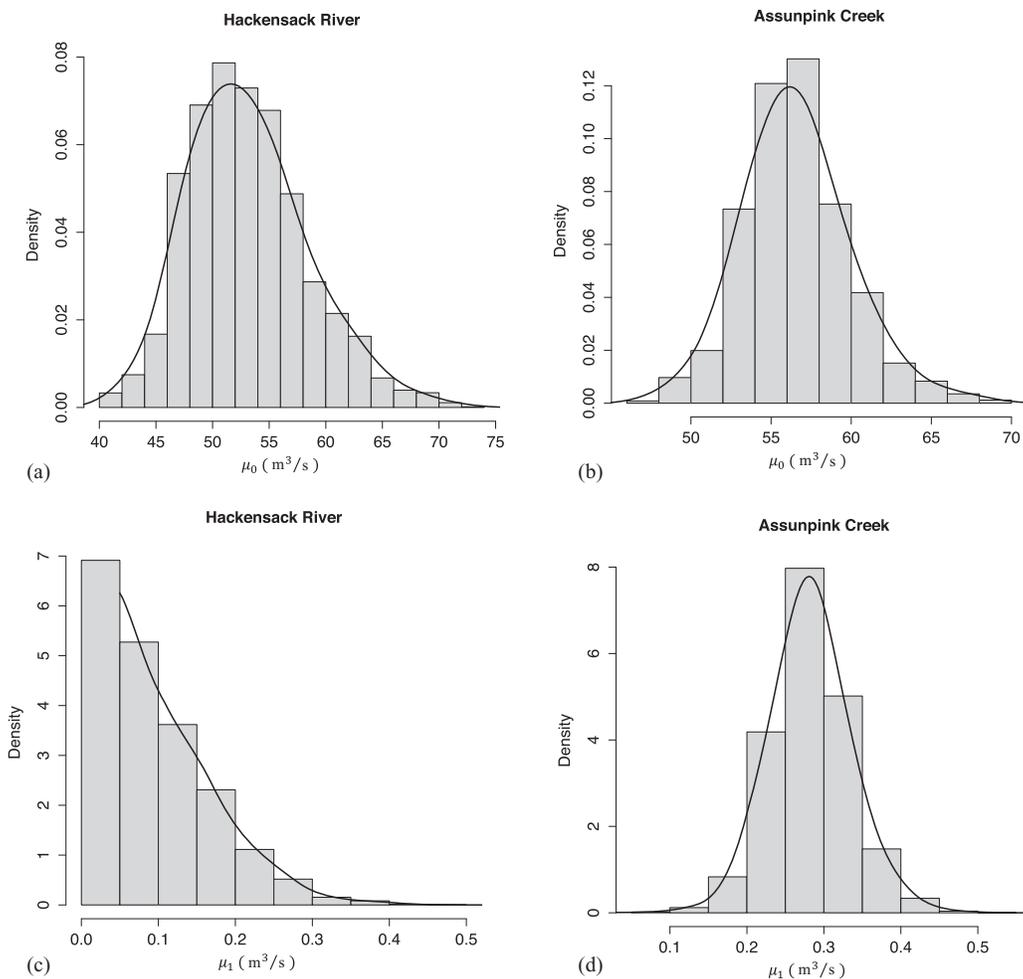
Fig. 4. Posterior distribution for parameters: (a) location intercept parameter for Hackensack River; (b) location intercept parameter for Assunpink Creek; (c) location slope parameter for Hackensack River; and (d) location slope parameter for Assunpink Creek.

In some parts of the USA, these flows show an increasing trend with time. Data for the Hackensack River at New Milford and for the Assunpink Creek watershed at Trenton [shown in Fig. 2 (Google 2019)] are two such examples in the state of New Jersey. The Assunpink Creek data have also been examined by Obeysekera and Salas (2014, 2016).

The annual peak flow data for the period 1924–2015 for these locations (Hackensack River station ID 01378500 and Assunpink Creek station ID 01464000) were obtained from the US Geological Survey website (USGS 2017). The extreme flow is plotted as a function of time for both datasets in Fig. 3, along with the line of best fit. The values of p for the slope of these lines are significantly less than 5%, as shown in the figure, suggesting the use of a nonstationary model for analysis. We used a nonstationary GEV model with a linear trend in the location parameter. We arbitrarily set the design year to be 2018 in both cases, since it is the year when this computational study was performed.

We applied the SC-BM method to both datasets. In all, 10,000 samples were collected for each of the parameters. For comparison, we also implemented the alternative methods: the traditional (i.e., unconstrained) maximum likelihood technique (MLE), a constrained maximum likelihood technique (C-MLE), and the traditional (i.e., unconstrained) Bayesian method (UC-BM) with no nonnegativity constraint on the location slope. Here, the unconstrained MLE is the typical estimate we reviewed earlier. In the C-MLE, the likelihood function (Eq. (4)) is solved while subjecting the slope parameter to

the nonnegative constraint. The inclusion of UC-BM in the comparison is to highlight the impact of the prior and the sign constraint. All the methods were implemented in R software (version 3.4.3).

We used uniform priors for both case studies. The advantage of using uniform priors is that they are uninformative, i.e., they allocate equal probabilities to all the values within the selected domain for the uniform distribution and thus do not favor any particular value of the parameter over others. However, if some information is available about the parameters, we can use some other prior distribution that assigns unequal probabilities to different values of the parameters, e.g., the normal distribution. Apart from allocating a uniform prior, we also need to constrain the sign of some of the parameters. We know that the flow volume of a river and its variance cannot be negative; thus, the location intercept parameter and the scale parameter must be restricted to positive values. This is done by setting the lower bound of the uniform prior to zero. If we wanted to use a normal prior, this sign constraint could have been applied by using the truncated normal distribution to discard all the negative values. Unlike the location intercept and the scale parameter, there is no reason to assume that the location slope parameter will always be positive. However, a negative location slope parameter does not have any significance from a design perspective. As explained previously, a negative value of the location slope parameter will drive the return period to ∞, which is not meaningful. If the location slope parameter for extreme flow for a river is negative, we would still design any structure at the current
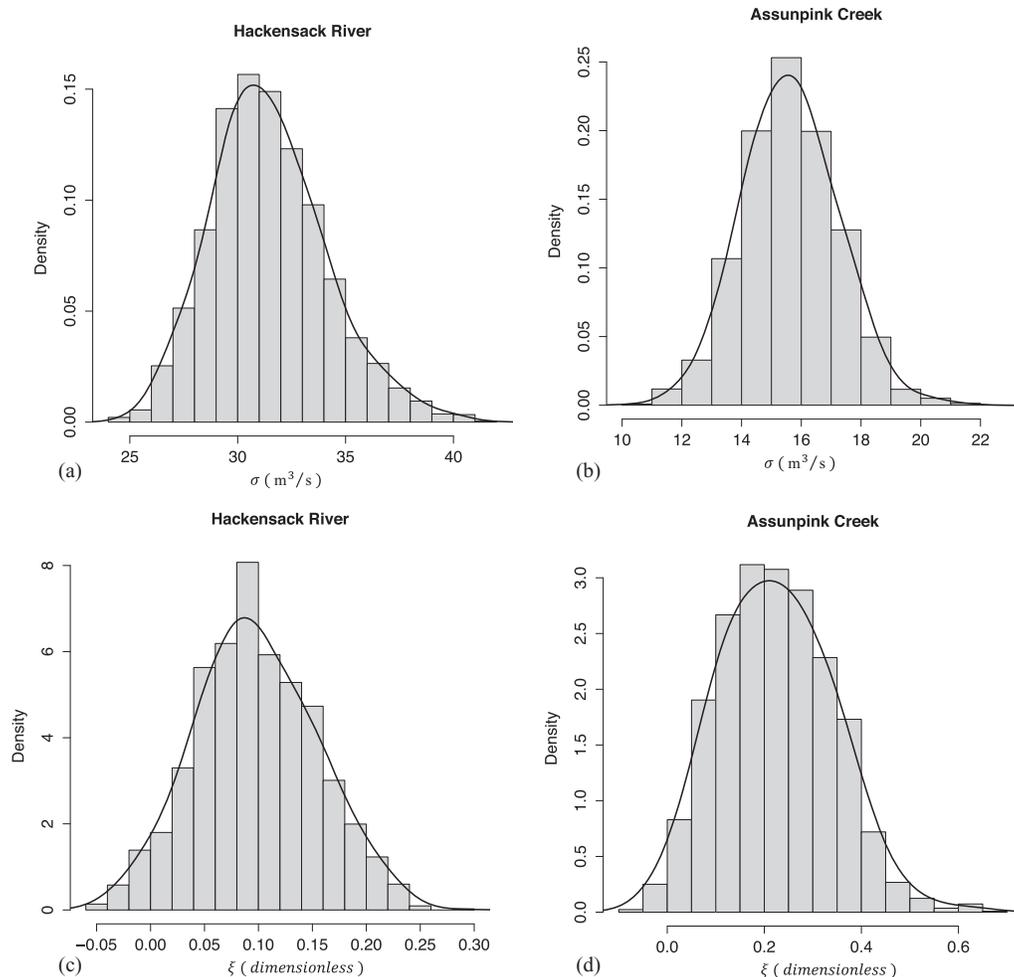
Fig. 5. Posterior distribution for parameters: (a) scale parameter for Hackensack River; (b) scale parameter for Assunpink Creek; (c) shape parameter for Hackensack River; and (d) shape parameter for Assunpink Creek.
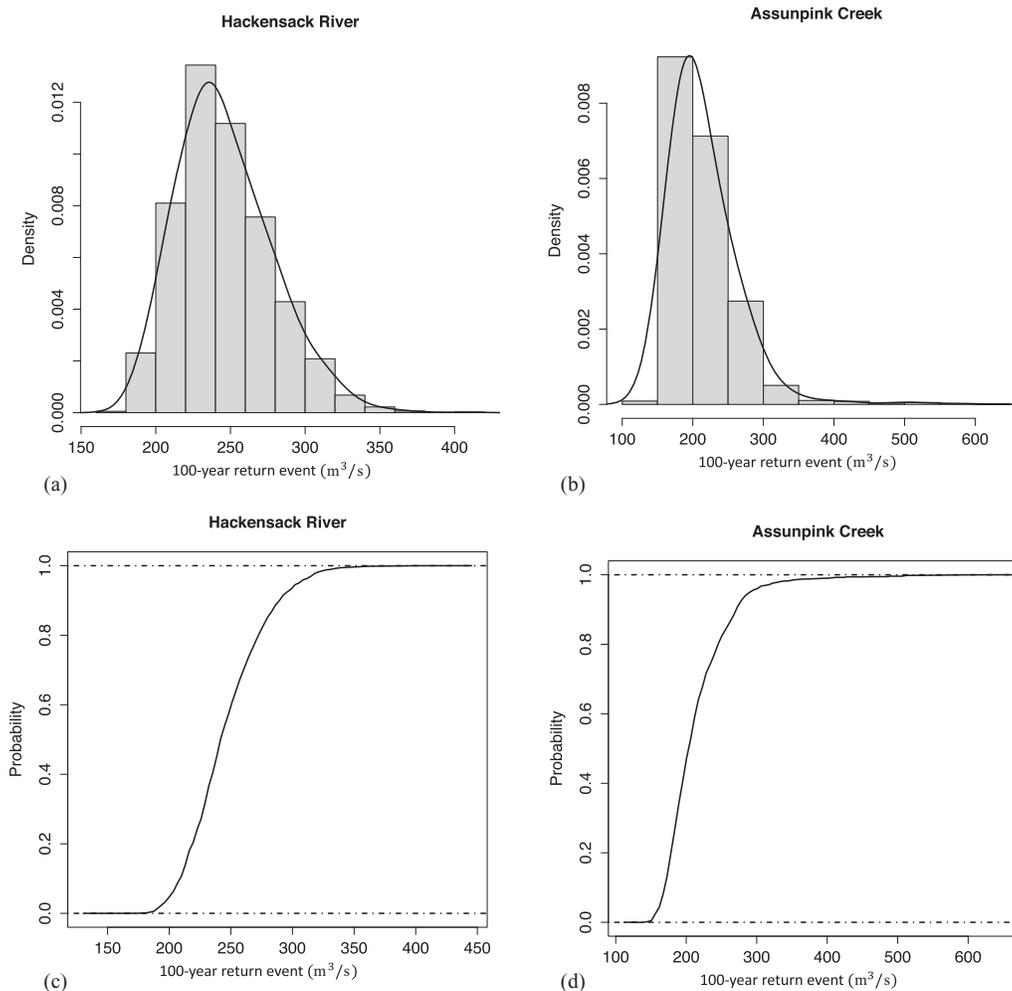
Fig. 6. Results for the 100 year return event: (a) posterior distribution for Hackensack River; (b) posterior distribution for Assunpink Creek; (c) CDF for Hackensack River; and (d) CDF for Assunpink Creek.

level of extreme flows. Moreover, uncertainty is involved in the parameter estimation. This implies that even when the most probable estimate of the location slope parameter is negative, there can still be a reasonable probability for the parameter to be positive. Thus, to get meaningful estimates for the design quantile, we propose the SC-BM, in which we also constrain the location slope parameter to be positive by setting the lower bound for its prior to zero. If the location slope parameter were most likely to take a negative value, this nonnegativity constraint in the SC-BM would ensure that the posterior distribution has its peak at zero.

The Metropolis-Hastings algorithm was used to draw samples from the posterior distribution of the parameters. Table 1 gives the specifications that were used in the MCMC algorithm. The proposal widths for the parameters were selected through experimentation to ensure a reasonable convergence rate for both datasets.

We report the estimated parameters, the 100 year return value, and the negative log-likelihood (NLLH) value for the alternative methods in Tables 2 and 3. (We only calculated the return event for the methods that gave nonnegative values of the location slope. We include the NLLH values in the tables as an indicator of goodness of fit between the resulting model and the data.) In spite of the peak flows showing an increasing trend in both cases (Fig. 3), the MLE of the location parameter of the nonstationary GEV model indicates a negative trend (i.e., negative μ_1) for the Hackensack River, but a positive trend for Assunpink Creek. It is

Table 4. Point estimates and confidence intervals

Dataset	Expected value	MAP value	95% CI
Assunpink Creek	214.3	195.2	[156.8, 322.1]
Hackensack River	246.2	235.7	[194.1, 316.9]

this issue that is the crux of this paper. The remainder of Tables 2 and 3 are discussed later.

The posterior distributions of the location intercept (μ_0) and slope (μ_1) parameters for the nonstationary GEV model are shown in Fig. 4. Even though a weak prior (uniform distribution over a large range) was used for the learning process, the posterior distributions of the parameters converged to reasonably concentrated distributions with low variance. Instead of simply having a point estimate, as in the MLE method, the Bayesian approach provides a distribution of the estimates. Figs. 4(a and b) show standard distributions for the location intercept parameter for the Hackensack River and Assunpink Creek, respectively. In Figs. 4(c and d), however, it is interesting to see how the distributions for the location slope parameter for the two streams are different. Owing to the use of the nonnegativity sign constraint, the shape of the distribution for the Hackensack data set looks like a truncated normal distribution instead of taking a standard shape. Indeed, this constrains the expected value of the slope parameter to be positive, as desired.

© ASCE

04020029-7

J. Waterway, Port, Coastal, Ocean Eng.

The posterior distributions for the scale (σ) and shape (ξ) parameters are shown in Fig. 5. Again, even though a weak prior was used for the learning process, the posterior distributions of these parameters also converged to a reasonably concentrated distributions with low variance. Both Figs. 5(a and b) and Figs. 5(c and d) show standard distributions for the scale and shape parameters for both streams.

Plots of the posterior distribution of a 100 year return event including the corresponding CDF for each dataset are shown in Fig. 6. The peak of the posterior distribution is known as the *maximum a posteriori* (MAP) estimate, which is the same as the expected value of an estimated parameter if the resulting distribution is symmetric. We can see that, in both datasets, the distribution of the 100 year return event is skewed and, therefore, the MAP estimate can be different from the expected estimate.

Returning to Tables 2 and 3, we can nominally use the NLLH to compare models; the smaller it is, the better is the model fit. In Table 2, we can see that the slope parameter estimates of all methods have comparable NLLH values. The unconstrained MLE is usually the model of the best fit, although with only a slightly lower NLLH value. However, in Table 2, it can be seen that it trades this superiority for a negative slope parameter. What this reveals is that a purely data-driven method does not always produce reasonable results, if not guided by domain knowledge of the underlying phenomenon. When a constraint is imposed on the slope parameter, as in the case of C-MLE, the resulting estimate of μ_1 is zero. This means that using this set of parameters for design yields the same result as using a stationary GEV distribution, and will therefore overlook the trend in the underlying events.

When the Bayesian method is applied without the sign constraint, it behaves in a manner similar to the MLE (a negative slope parameter in Table 2), demonstrating that reliance on the Bayesian method itself is not sufficient; imposing a nonnegativity restriction on the parameter via the prior is necessary. Further analysis of the results shows that when MLE returns a positive slope estimate (Table 3), the SC-BM produces estimates similar to those of the other methods. However, when MLE returns a negative slope estimate (Table 2), the SC-BM provides the best estimate, compared with the unconstrained methods (MLE and UC-BM) as well as compared with the alternative constrained method (C-MLE).

A further benefit of using the Bayesian method is that uncertainty quantification is a natural outcome of using the resulting posterior distribution. The histograms for the 100 year return events for both datasets show a highly peaked mode and are right skewed; this suggests that the expected value would be greater than the MAP value. The expected value, the MAP value, and the 95% confidence interval (CI) for the 100 year return event are reported in Table 4. It can be seen that expected values are indeed greater than MAP values. If the aim is to design a structure, one might prefer the expected value over the MAP value of the return event. These distributions can be used by a designer to understand the uncertainty involved in the design quantile and quantify the risk.

Summary and Conclusions

Hydrological extreme events are often the major cause of failure of many civil engineering structures. Hence, quantifying the extreme events in terms of design quantiles becomes a crucial task. Probabilistic models are used to analyze these extreme events. This work considers a sign constrained Bayesian method for performing parameter estimation in a nonstationary GEV model. We show that one can encounter a negative slope in the location parameter even though the trend in the data may be positive. The modification of the traditional Bayesian method is capable of handling such datasets

and produces the posterior distribution of the parameters based on the observed data and not point estimates. Thus, this provides a needed basis for uncertainty quantification. Further, the availability of a probability distribution for the return event gives the engineering designers and planners additional information and perspective on the risks involved with a given design quantile.

The results based on two case studies demonstrate that the SC-BM works as a unified framework to handle different classes of problem. When the MLE technique produces a positive location slope parameter value, the SC-BM produces results comparable to MLE. However, when MLE returns a negative estimate of the location slope parameter in spite of an increasing trend in the data, the SC-BM corrects this estimation problem and produces a trend estimate consistent with data. It is hoped that the sign constrained Bayesian method will assist practitioners in incorporating climate-related trends to estimate design conditions.

Data Availability Statement

- Some or all data, models, or code generated or used during the study are available in a repository or online in accordance with funder data retention policies (USGS 2017).
- Some or all data, models, or code generated or used during the study are available from the corresponding author by request: R software codes for SC-BM and UC-BM algorithms.

References

Caires, S., V. Swail, and X. Wang. 2006. "Projection and analysis of extreme wave climate." *J. Clim.* 19 (21): 5581–5605. https://doi.org/10.1175/JCLI3918.1.

Coles, S. 2001. *An introduction to statistical modeling of extreme values*. London: Springer.

Cox, R. T. 1946. "Probability, frequency and reasonable expectation." *Am. J. Phys.* 14 (1): 1–13. https://doi.org/10.1119/1.1990764.

Cox, R. T. 1961. *The algebra of probable inference*. Baltimore: Johns Hopkins.

Das, J., and N. Umamahesh. 2017. "Uncertainty and nonstationarity in streamflow extremes under climate change scenarios over a river basin." *J. Hydrol. Eng.* 22 (10): 04017042. https://doi.org/10.1061/(ASCE)HE.1943-5584.0001571.

De Paola, F., M. Giugni, F. Pugliese, A. Annis, and F. Nardi. 2018. "GEV parameter estimation and stationary vs. non-stationary analysis of extreme rainfall in African test cities." *Hydrology* 5 (2): 28. https://doi.org/10.3390/hydrology5020028.

De Paola, F., M. Giugni, M. E. Topa, and E. Bucchignani. 2014. "Intensity-Duration-Frequency (IDF) rainfall curves, for data series and climate projection in African cities." *SpringerPlus* 3 (1): 133. https://doi.org/10.1186/2193-1801-3-133.

Douglas, E. M., R. M. Vogel, and C. N. Kroll. 2000. "Trends in floods in the United States: Impact of spatial correlation." *J. Hydrol.* 240 (1–2): 90–105. https://doi.org/10.1016/S0022-1694(00)00336-X.

Gado, T. A., and V.-T.-V. Nguyen. 2016. "An at-site flood estimation method in the context of nonstationarity I. A simulation study." *J. Hydrol.* 535: 710–721. https://doi.org/10.1016/j.jhydrol.2015.12.063.

Google. 2019. "Map for Assunpink Creek (lattitude: 40.22416; longitude: -74.74916), and Hackensack River (lattitude: 40.94833, longitude: -74.02666)." Accessed August 23, 2019. https://maps.google.com.

Haan, L. D., and A. Ferreira. 2006. *Extreme value theory an introduction*. New York: Springer.

Hastings, W. K. 1970. "Monte Carlo sampling methods using Markov chains and their applications." *Biometrika* 57 (1): 97–109. https://doi.org/10.1093/biomet/57.1.97.

Hoff, P. D. 2009. *A first course in Bayesian statistical methods*. New York: Springer.

Lins, H. F., and J. R. Slack. 1999. "Streamflow trends in the United States." *Geophys. Res. Lett.* 26 (2): 227–230. https://doi.org/10.1029/1998GL900291.

Masina, A., and A. Lamberti. 2013. "A nonstationary analysis for the northern adriatic sea levels." *J. Geophys. Res.* 118 (9): 3999–4016. https://doi.org/10.1002/jgrc.20313.

Metropolis, N., A. W. Rosenbluth, M. N. Rosenbluth, A. H. Teller, and E. Teller. 1953. "Equation of state calculations by fast computing machines." *J. Chem. Phys.* 21 (6): 1087–1092. https://doi.org/10.1063/1.1699114.

Mood, A., F. Graybill, and D. Boes. 1974. *Introduction to the theory of statistics*. 3rd ed. New York: McGraw-Hill.

Mudersbach, C., and J. Jensen. 2010. "Nonstationary extreme value analysis of annual maximum water levels for designing coastal structures on the German North Sea coastline." *J. Flood Risk Manage.* 3 (1): 52–62. https://doi.org/10.1111/jfrm.2010.3.issue-1.

Obeysekera, J., J. Park, M. Irizarry-Ortiz, J. Barnes, and P. Trimble. 2013. "Probabilistic projection of mean sea level and coastal extremes." *J. Waterway, Port, Coastal, Ocean Eng.* 139 (2): 135–141. https://doi.org/10.1061/(ASCE)WW.1943-5460.0000154.

Obeysekera, J., and J. D. Salas. 2014. "Quantifying the uncertainty of design floods under nonstationary conditions." *J. Hydrol. Eng.* 19 (7): 1438–1446. https://doi.org/10.1061/(ASCE)HE.1943-5584.0000931.

Obeysekera, J., and J. D. Salas. 2016. "Frequency of recurrent extremes under nonstationarity." *J. Hydrol. Eng.* 21 (5): 04016005. https://doi.org/10.1061/(ASCE)HE.1943-5584.0001339.

Olsen, J. R., J. R. Stedinger, N. C. Matalas, and E. Z. Stakhiv. 1999. "Climate variability and flood frequency estimation for the upper Mississippi and lower Missouri rivers." *J. Am. Water Resour. Assoc.* 35 (6): 1509–1523. https://doi.org/10.1111/jawr.1999.35.issue-6.

Potter, K. W. 1991. "Hydrologic impacts of changing land management practices in moderate-sized agriculture catchments." *Water Resour. Res.* 27 (5): 845–855. https://doi.org/10.1029/91WR00076.

Salas, J. D., and J. Obeysekera. 2014. "Revisiting the concepts of return period and risk for nonstationary hydrologic extreme events." *J. Hydrol. Eng.* 19 (3): 554–568. https://doi.org/10.1061/(ASCE)HE.1943-5584.0000820.

Savage, L. J. 1972. *The foundations of statistics*. Revised ed. New York: Dover.

Strupczewski, W. G., V. P. Singh, and H. T. Mitosek. 2001a. "Nonstationary approach to at-site flood frequency modeling. I. Maximum likelihood estimation." *J. Hydrol.* 248 (1–4): 123–142. https://doi.org/10.1016/S0022-1694(01)00397-3.

Strupczewski, W. G., V. P. Singh, and H. T. Mitosek. 2001b. "Nonstationary approach to at-site flood frequency modeling. III. Flood frequency analysis of Polish rivers." *J. Hydrol.* 248 (1–4): 152–167. https://doi.org/10.1016/S0022-1694(01)00399-7.

USGS (US Geological Survey). 2017. "USGS peak streamflow for the nation." Accessed December 25, 2017. https://waterdata.usgs.gov/nwis/peak.